Supporting Information

Do [all]-*S,S´*-Dioxide Oligothiophenes Show Electronic and Optical Properties of Oligoenes and/or of Oligothiophenes?

María Moreno Oliva, Juan Casado, Juan T. López Navarrete**

Department of Physical Chemistry, University of Málaga, Campus de Teatinos s/n, Málaga 29071, Spain

Serguei Patchkovskii

Steacie Institute for Molecular Sciences, National Research Council of Canada, 100 Sussex Drive, Ottawa, K1A 0R6 Canada

Theodore Goodson III, Michael R. Harpham

Department of Chemistry, University of Michigan, Ann Arbor, Michigan 48109, USA

J. Sérgio Seixas de Melo

Department of Chemistry, University of Coimbra, 3004-535 Coimbra, Portugal

Elizabeta Amir, Shlomo Rozen

School of Chemistry, Raymond and Beverly Sackler Faculty of Exact Sciences, Tel-Aviv University, Tel-Aviv 69978, Israel

***To whom correspondence should be addressed. E-mail: (J.C.)** casado@uma.es, **teodomiro@uma.es**

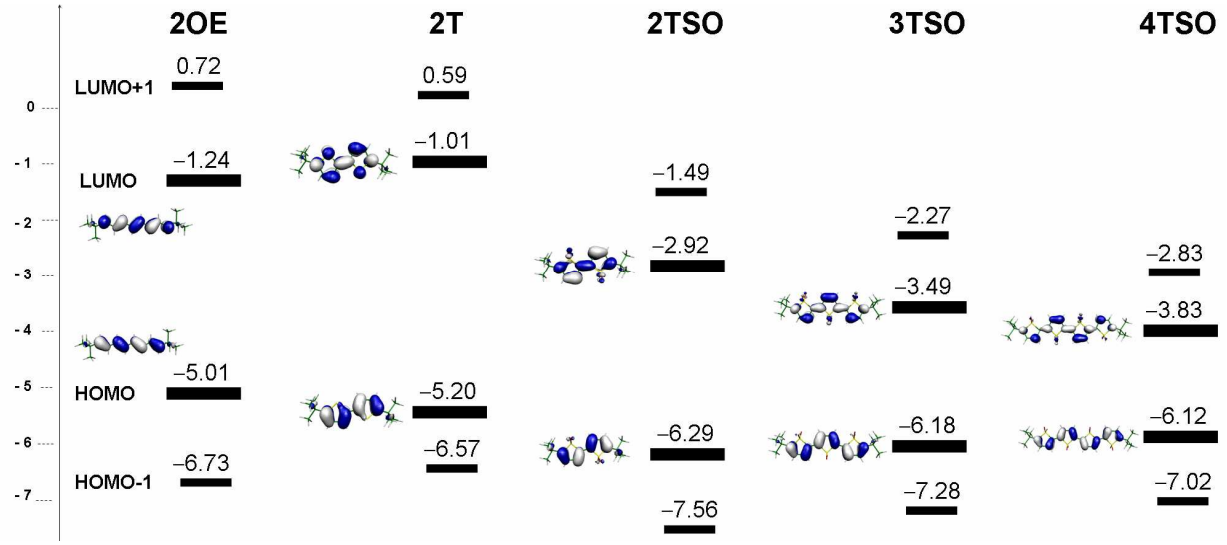

Figure S1. DFT//B3LYP/6-31G** energies of the orbital terms around the gap together with their wavefunctions topologies.

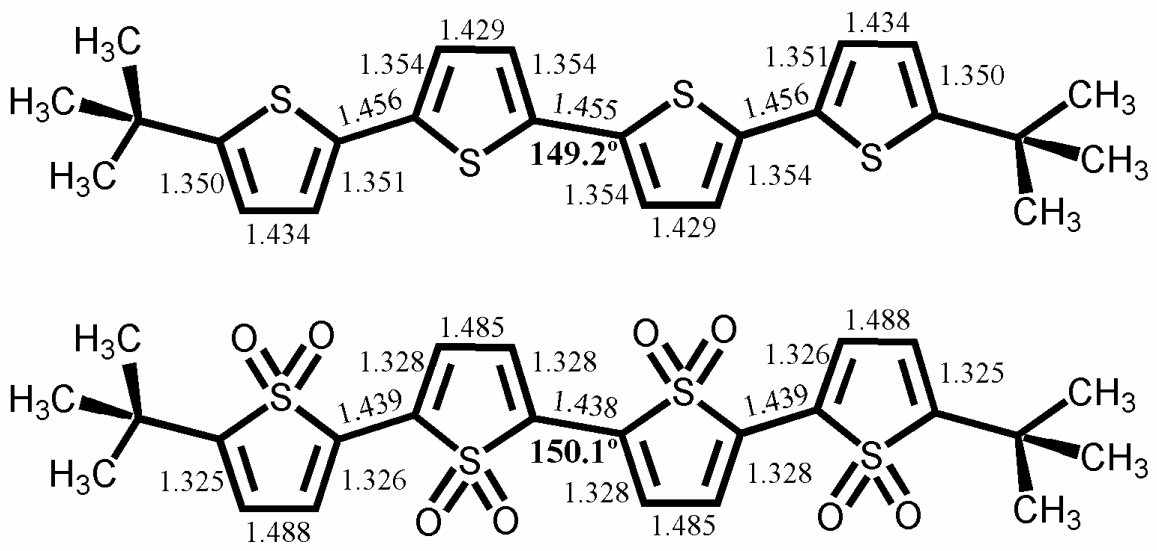

Figure S2. RCIS/HF/3-21G* optimized geometries of the ground electronic state of **4T** and **4TSO**.

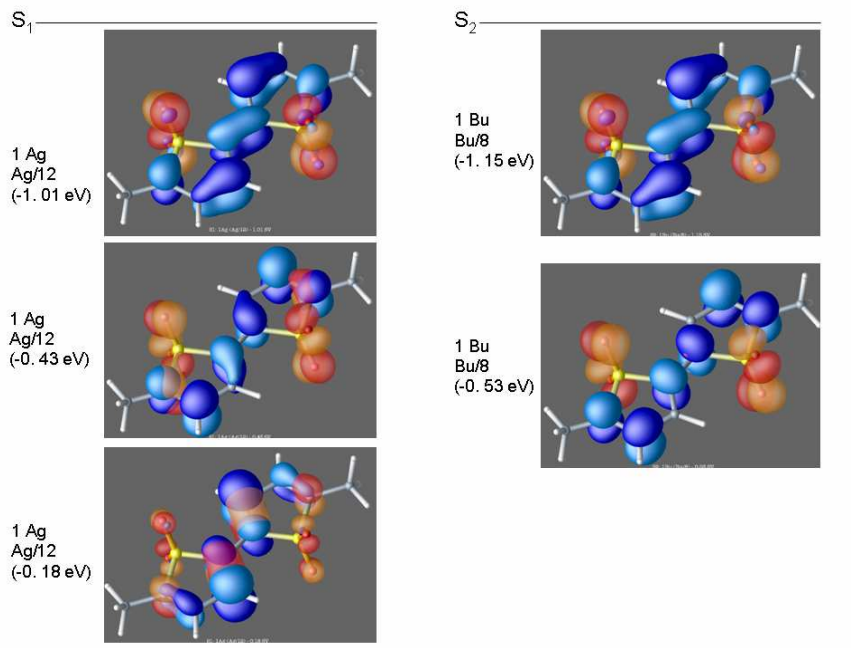

Figure S3. MCQDPT2 pictures of the orbitals contributing to S_1 and S_2 singlet excitations in **2TSO**.

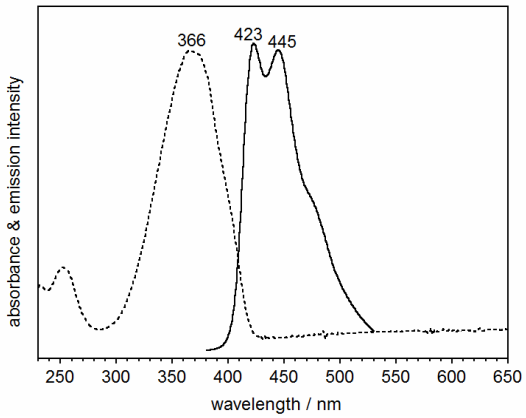

Figure S4. Absorption and emission spectra of **3T** at 25ºC in dichloromethane.

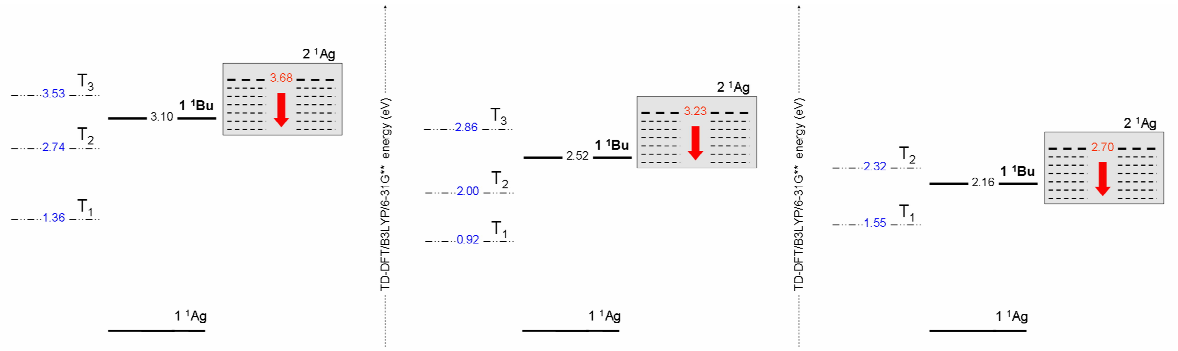

Figure S5. Energy diagram showing the singlet and triplet manifold according to TD-DFT//B3LYP/6-31G** calculations in **2TSO** (left), **3TSO** (middle) and in **4TSO** (right). In the boxes, the effect of electron correlation is tried to be described producing a stabilization of the 2 ^{1}Ag state.

Table S1. Physical properties of the solvents. [a)]

Solvent	ϵ	μ (D)	Polarity (SPP)	Viscosity (mPa s)
Butyronitrile	20.7	-----	0.915	0.57
Ethanol	24.3	1.7	0.853	1.20
DCM	8.9	1.1	0.876	0.44
THF	7.6	1.7	0.838	0.47
Toluene	2.4	0.3	0.655	0.58
Decaline	2.2	≈ 0	0.574	2.7

[a)] The solvent polarity is expressed in the solvent polarity polarizability (SPP) scale.

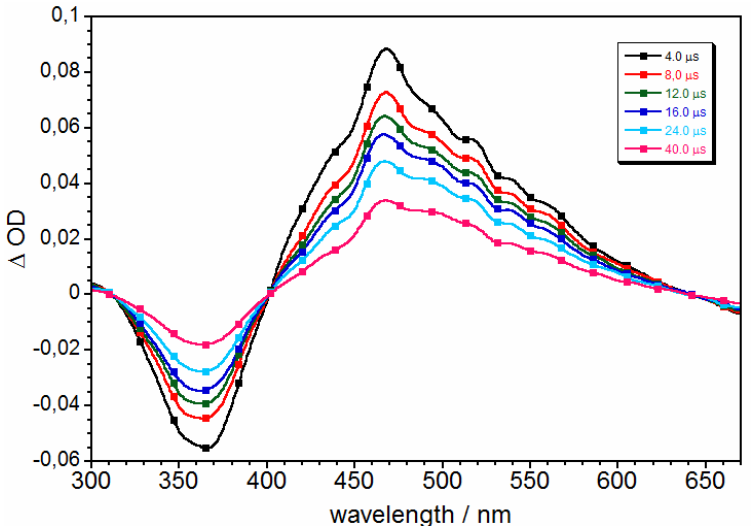

Figure S6. Transient triplet-triplet spectra of **3T** in ethanol at room temperature (25ºC).

Table S2. Photophysical parameters and rate constants in ethanol.

	Φ_F	τ_F [ns]	Φ_Δ	Φ_T	k_T [s^{-1}]	τ_T [s]	k_F [ns^{-1}]	k_{NR} [ns^{-1}]	k_{ISC} [ns^{-1}]	k_{IC} [ns^{-1}]
3T	0.07	0.19	0.84	0.91	$2.72 \cdot 10^4$	$3.68 \cdot 10^{-5}$	0.37	4.89	4.80	0.11
3TSO	0.004	0.22 (53%) 0.82 (47%)	0.01	-	-	-	-	-	-	-

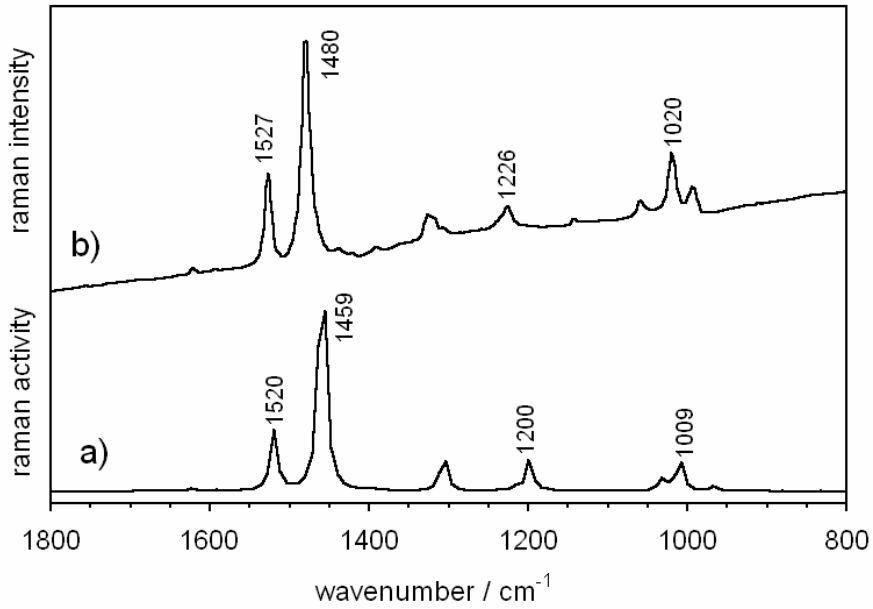

Figure S7. a) DFT//B3LYP/6-31G** theoretical Raman and b) experimental 1064 nm FT-Raman spectra of **4TSO**.

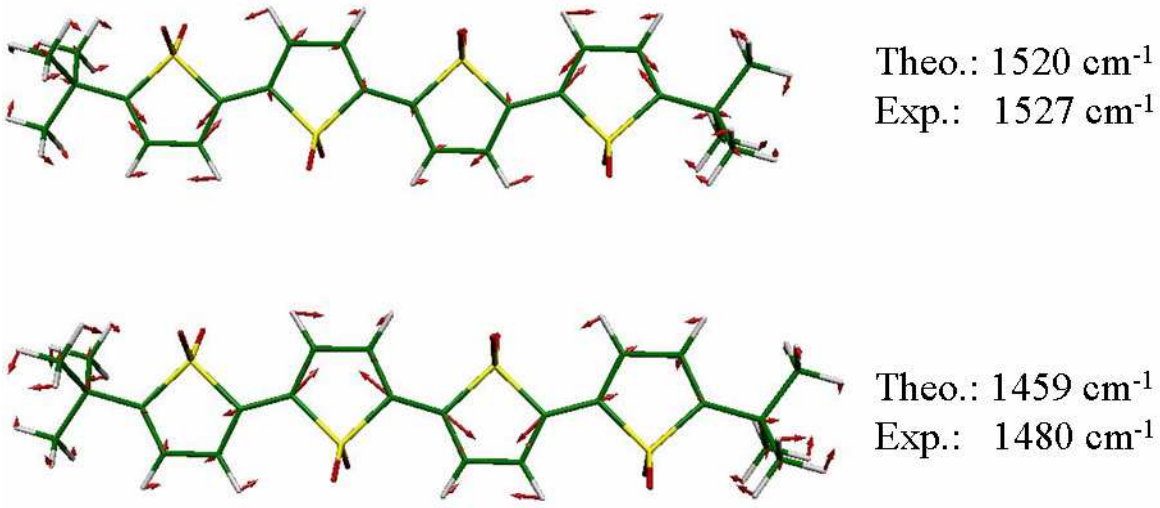

Figure S8. DFT//B3LYP/6-31G** vibrational eigenvectors associated with the most important Raman lines.

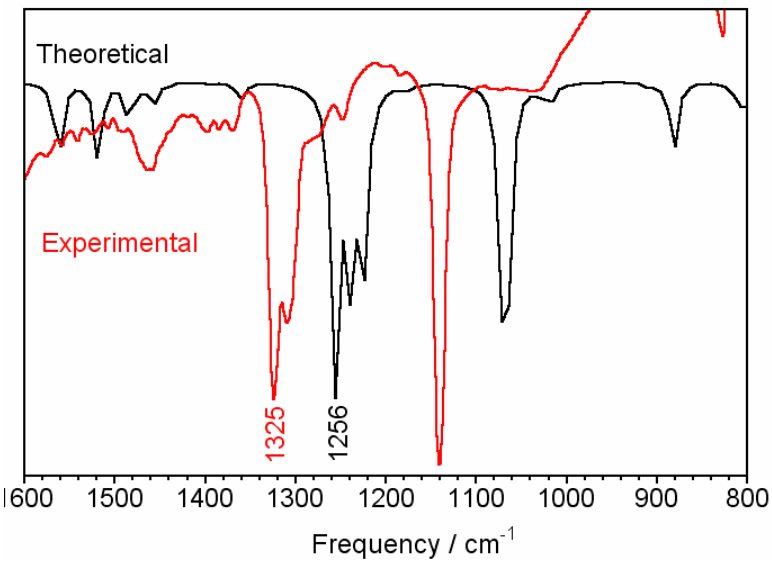

Figure S9. DFT//B3LYP/6-31G** theoretical and experimental infrared spectra of **4TSO**.

Figure S10. DFT//B3LYP/6-31G** vibrational eigenvector associated with the ν(S–O) most intense infrared bands.

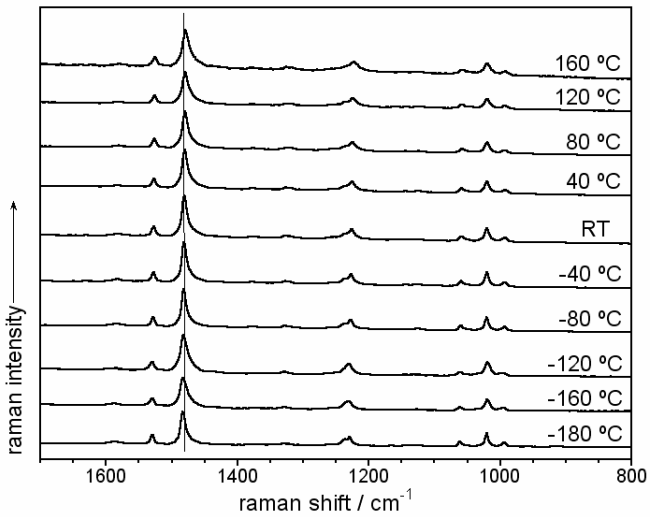

Figure S11. 532 nm FT-Raman spectra in solid state of **4TSO** at high and low temperatures. Raman thermo-spectroscopy was carried out in a Limkan cell equipped for the Senterra Raman spectrometer microscope.

Experimental and theoretical details

The chemical synthesis of the studied compounds has been previously published elsewhere.[1] The data presented in this paper for the oligoenes are those available in the literature.[2] UV-Vis absorption spectra were recorded on an Agilent 8453 instrument equipped with a diode array detection system. Emission spectra were measured using a spectrofluorometer from Edinburgh Analytical Instrument (FLS920P) equipped with a pulsed xenon flash-lamp. Fluorescence decays were measured using a Single Photon Photomultiplier Detection System (S900) with Picosecond Pulsed Diode Laser (PDL 800-B), from Edinburgh Instruments. For low temperature studies, an OptistatDN Cryostat was used. All solvents used were of spectroscopic grade from Aldrich. Fluorescence quantum yields, ϕ_F, were measured for all the solutions using 1 x 10^{-7} mol L^{-1} quinine sulfate in 0.1 mol L^{-1} H_2SO_4 as the standard (ϕ_F=0.546). No fluorescent contaminants were detected upon excitation in the wavelength region of experimental interest.

The two-photon excited fluorescence (TPEF) method was employed to evaluate the two-photon absorption cross-sections (TPACS) of the samples.[3,4] The TPACS was evaluated over the excitation wavelength range of 710-900 nm using a mode-locked Ti:sapphire laser (Spectra-Physics MaiTai® HP, pulsewidth < 100 fs, 80 MHz repetition rate). In applying the TPEF technique, two-photon absorption cross-sections were measured relative to a reference solution of Rhodamine B (prepared at pH 10) in methanol at known concentration. TPACS for a specific excitation wavelength were evaluated at the emission wavelength corresponding to the maximum in the TPEF spectrum.

FT-Raman scattering spectra with excitation at 1064 nm were collected on a Bruker FRA106/S apparatus and a Nd:YAG laser source (λ_{exc} = 1064 nm), in a back-scattering configuration. The operating power for the exciting laser radiation was kept to 100 mW in all the experiments. Samples were analyzed as pure solids averaging 1000 scans with 2 cm^{-1} of

spectral resolution. Raman spectra (λ_{exc} = 532 nm, 633 nm, 785 nm) were recorded by using a Senterra dispersive Raman microscope from Bruker whereas the Raman spectrum with the 488 nm excitation wavelength was obtained using a Microscope Invia Reflex Raman RENISHAW.

Ground state total energies, equilibrium geometries, eigenfrequencies, and normal coordinates were calculated using Density Functional Theory (DFT) by means of the GAUSSIAN-03 programming package.[5] The Becke's three parameter (B3) gradient-corrected exchange functional combined with the correlation Lee-Yang-Parr (LYP) correlation functional was utilized.[6] The 6-31G** basis set was used.[7] Theoretical Raman spectra were obtained for the resulting ground-state optimized geometries. Harmonic vibrational frequencies and Raman intensities were calculated analytically and numerically respectively.[8] The time-dependent DFT (TD–DFT) approach has been used for the evaluation of, at a minimum, the ten lowest-energy vertical electronic excited states including both singlet and triplet states.[9] TD–DFT calculations were performed using the same functional (B3LYP) and basis set (6-31G**). Excited state optimized geometries were assesed with the restricted single excited configuration interaction approach (CIS) within the Hartree-Fock (HF) approximation, or RCIS/HF.[10] Within this framework, a single determinant RHF wavefunction is used as the reference determinant in a CIS calculation of excited states.

Furthermore, **2T** and **2TSO** ground-state geometries, constrained to the C_{2h} point-group symmetry, were optimized using MP2(fc)/cc-Pvdz[11] level of theory and basis set. The low-lying singlet excited states for the resulting structures were calculated using occupation-restricted multiple active space multi-configurational self-consistent field wavefunctions (ORMAS MCSCF)[12], including second-order quasi-degenerate multiconfigurational perturbation theory (MCQDPT2) [13] corrections for the state energies. Restricted active space was partitioned into the occupied and virtual spaces, with up to three electrons in the virtual

space. The occupied and virtual spaces were adjusted until the external singles and doubles MCQDPT2 contributions to the excited states of interest were below 40% and the ordering of the 8 lowest MCQDPT2 singlets has converged. In **2T**, the final active space was optimized for the 13 equally-weighed singlets and contained 6 occupied (a_u^3 b_g^3) and 9 virtual (a_u^2 a_g^2 b_g^2 b_u^3) orbitals. In **2TSO**, MCSCF optimization included 15 equally-weighted singlets, with 7 occupied (a_u^3 a_g^1 b_g^3) and 9 virtual (a_u^3 a_g^1 b_g^3 b_u^2) orbitals. As a convergence check, the **2TSO** MCSCF optimization was repeated for 20 lowest singlets, with the virtual space expanded to 12 orbitals (a_u^3 a_g^3 b_g^3 b_u^3).

[1]. Amir, E.; Rozen, S. *Angew. Chem. Int. Ed*. **2005**, *44*, 7374.

[3]. Xu, C.; Webb, W. W. *J. Opt. Soc. Am. B-Opt. Phys.* **1996**, *13*, 481.

[4]. Makarov, N. S.; Drobizhev, M.; Rebane, A. *Opt. Expr.* **2008**, *16*, 4029.

[5]. Gaussian 03, Revision C.02, Frisch, M. J.; Trucks, G. W.; Schlegel, H. B.; Scuseria, G. E.; Robb, M. A.; Cheeseman, J. R.; Montgomery, Jr., J. A.; Vreven, T.; Kudin, K. N.; Burant, J. C.; Millam, J. M.; Iyengar, S. S.; Tomasi, J.; Barone, V.; Mennucci, B.; Cossi, M.; Scalmani, G.; Rega, N.; Petersson, G. A.; Nakatsuji, H.; Hada, M.; Ehara, M.; Toyota, K.; Fukuda, R.; Hasegawa, J.; Ishida, M.; Nakajima, T.; Honda, Y.; Kitao, O.; Nakai, H.; Klene, M.; Li, X.; Knox, J. E.; Hratchian, H. P.; Cross, J. B.; Bakken, V.; Adamo, C.; Jaramillo, J.; Gomperts, R.; Stratmann, R. E.; Yazyev, O.; Austin, A. J.; Cammi, R.; Pomelli, C.; Ochterski, J. W.; Ayala, P. Y.; Morokuma, K.; Voth, G. A.; Salvador, P.; Dannenberg, J. J.; Zakrzewski, V. G.; Dapprich, S.; Daniels, A. D.; Strain, M. C.; Farkas, O.; Malick, D. K.; Rabuck, A. D.; Raghavachari, K.; Foresman, J. B.; Ortiz, J. V.; Cui, Q.; Baboul, A. G.; Clifford, S.; Cioslowski, J.; Stefanov, B. B.; Liu, G.; Liashenko, A.; Piskorz, P.; Komaromi, I.; Martin, R. L.; Fox, D. J.; Keith, T.; Al-Laham, M. A.; Peng, C. Y.; Nanayakkara, A.;

Challacombe, M.; Gill, P. M. W.; Johnson, B.; Chen, W.; Wong, M. W.; Gonzalez, C.; and Pople, J. A.; Gaussian, Inc., Wallingford CT, 2004.

[6]. Becke, A. D. *J. Chem. Phys.* **1993**, *98*, 1372.

[7]. Francl, M. M.; Pietro, W. J.; Hehre, W. J.; Binkley, J. S.; Gordon, M. S.; Defrees, D. J.; Pople, J. A. *J. Chem. Phys.* **1982**, *77*, 3654.

[8]. Scott, A. P.; Radom, L. *J. Phys. Chem.* **1996**, *100*, 16502.

[9]. Runge, E.; Gross, E. K. U. *Phys. Rev. Lett.* **1984**, *52*, 997; Gross, E. K. U.; Kohn, W. *Adv. Quantum Chem.* **1990**, *21*, 255; Heinze, H.; Goerling, A.; Roesch, N. *J. Chem. Phys.* **2000**, *113*, 2088.

[10]. Foresman, J.B.; Head-Gordon, M.; Pople, J.A.; Frish, M. J. *J. Phys. Chem.* **1992**, *96*, 135.

[11]. a) Schmidt, M.W.; Baldridge, K.K.; Boatz, J.A.; Elbert, S.T.; Gordon, M.S.; Jensen, J.J.; Koseki, S.; Matsunaga, N.; Nguyen, K.A.; Su, S.; Windus, T.L.; Dupuis, M.; Montgomery, J.A. *J.Comput.Chem.* **1993,** *14*, 1347. b) Gordon, M.S.; Schmidt, M.W. pp 1167-1189 in: Dykstra, C.E.; Frenking, G.; Kim, K.S.; Scuseria, G.E. (eds), *"Theory and Applications of Computational Chemistry, the first forty years",* (Elsevier, Amsterdam, 2005). c) Aikens, C.M.; Webb, S.P.; Bell, R.L.; Fletcher, G.D.; Schmidt, M.W.; Gordon, M.S. *Theor.Chem.Acc.* **2003** *110*, 233. d) Dunning Jr., T.H. *J. Chem. Phys.* **1989**, *90*, 1007.

[12]. a) Ivanic, J. *J. Chem. Phys*. **2003**, *119*, 9364. b) Ivanic, J. *J. Chem. Phys.* **2003**, *119*, 9377. c) Schmidt, M.W.; Gordon, M.S.; *Ann. Rev. Phys. Chem.* **1998**, *49*, 233.

[13]. a) Nakano, H.; Uchiyama, R.; Hirao, K. *J. Comput. Chem.* **2002**, *23*, 1166. b) Miyajima, M.; Watanabe, Y.; Nakano, H. *J.Chem.Phys.* **2006**, *124*, 044101. c) Ebisuzaki, R.; Watanabe, Y.; Nakano, H. *Chem. Phys. Lett.* **2007**, *442*, 164.

Additional Theoretical Details

Excited states calculations for thiophene and thiophene sulfoxide oligomers:

Geometries are optimized using MP2(fc)/cc-pVDZ. The optimized Cartesian coordinates are attached.

All structures are constrained to be planar (C_{2h} point group).

MP2 frequency calculation on 2T gives many soft modes, including:

68i cm^{-1} CH_3 torsion mode (2x)
37i cm^{-1} central C-C torsion mode
79 cm^{-1} out-of-plane overall bend

MP2 frequency run on 2TSO gives many soft modes as well, including:

162i cm^{-1} CH_3 torsion mode (2x)
<70i cm^{-1} central C-C torsion mode, mixed with overall rotations
45 cm^{-1} out-of-plane overall bend

CH_3 torsion modes could be resolved by rotating the groups 30 degrees. However, this would drop the symmetry to either Ci or nothing (depending on the sense of CH3 rotation).

Excited states are calculated using occupation-restricted multiple active space multi-configuratinal self-consistent field wavefunctions (ORMAS MCSCF), with second-order quasi-degenerate multiconfigurational perturbation theory (MCQDPT2) corrections for the state energies.

Restricted active space was partitioned into the occupied and virtual spaces, with up to three electrons in the virtual space. The occupied and virtual spaces were adjusted until the external singles and doubles MCQDPT2 contributions to the excited states of interest were below 40\%

1. Electronic structure of 2T

The final active space of the 2T molecule consisted of a 6-orbital occupied block (3*Au + 3*Bg irreducible representations) and a 9-orbital virtual block (2*Au + 2*Ag + 2*Bg + 3*Bu). The active space was optimized for the 13 equally-weighted singlet states.

As a check, the calculation using the same active space was repeated using cc-pVTZ basis set.

The lowest singlet excited states of 2T are (in eV).

cc-pVDZ states:

		MCQDPT2	MCSCF	##	Osc.Str.
1	Ag/1	0.000	0.000	1	
2	Bu/3	2.838	5.505	3	0.5303
3	Ag/8	4.454	7.748	10	
4	Ag/4	4.962	5.364	2	
5	Bu/8	4.983	8.119	11	0.4042
6	Ag/5	5.444	6.094	5	

7	Bg/2	5.455	6.228	6	
8	Au/2	5.532	6.331	7	0.0008
9	Au/4	6.557	6.919	8	0.0000
10	Bg/4	6.569	6.933	9	
11	Bu/9	6.820	8.257	13	0.0250
12	Bu/4	7.354	6.027	4	0.1804
13	Ag/10	7.787	8.186	12	

cc-pVTZ states:

		MCQDPT2	MCSCF	##	Osc.Str.
1	Ag/1	0.000	0.000	1	
2	Bu/3	2.628	5.454	3	0.4066
3	Ag/8	4.059	7.701	11	
4	Bu/8	4.837	8.107	12	0.4673
5	Ag/4	4.857	5.338	2	
6	Bg/2	5.179	5.973	4	
7	Au/2	5.222	6.060	6	0.0002
8	Ag/5	5.328	6.093	7	
9	Au/4	6.244	6.709	8	0.0003
10	Bg/4	6.326	6.731	9	
11	Au/6	6.587	7.586	10	0.0002
12	Bu/4	7.226	5.995	5	0.1060
13	Ag/10	7.729	8.172	13	

The two calculations show an excellent agreement for the lowest ten MCQDPT2 states.
The state energies agree to better than 0.4 eV between the two basis sets. The ordering of the states agrees closely as well, except for the interchange between quasi-degenerate 3Ag and 2Bu levels around 5.0 eV excitation energy, and the three-level nest of 6Ag, 1Bg, and 1Au levels at approximately 5.5 eV.

The calculated vertical excitation energies for the Ag states also agree quite well with previous CASPT2 calculation by Rubio. At the same time, there is a significant disagreement in the calculated positions of the dipole-allowed levels of Bu symmetry. We calculated the 1Bu level at approximately 2.84 eV (Rubio: 3.88 eV), with the 2Bu level at 4.98 eV (Rubio: 4.15 eV). In this respect, it has to be noted that states of Bu symmetry are highly sensitive to the size of the active space and the number of states included in the state average. In this work, a 15-orbital restricted active space was necessary to achieve the convergence. Preliminary calculations with smaller active spaces show a better agreement to the results of Rubio et al, who used a 10-orbital complete active space.

In order characterize the nature of excited states, we calculated the reduced one-particle transition density matrix (1-TRDM) for the excitation from the ground state to the seven lowest excited states. In all cases, the MCSCF wavefunctions were used, so that the 1-TRDM should be treated as semi-quantitative.

	State	MCQDPT2	1-TRDM trace	1-TRDM singular values > 0.1				
				1	2	3		
1	Ag/1	0.000						
2	Bu/3	2.838	2.13	1.20	0.31	0.22	0.16	0.12
3	Ag/8	4.454	2.26	0.79	0.76	0.27	0.12	
4	Ag/4	4.962	1.80	0.68	0.65	0.14	0.11	
5	Bu/8	4.983	1.88	1.01	0.40	0.22		
6	Ag/5	5.444	1.95	1.04	0.36	0.21	0.13	
7	Bg/2	5.455	1.65	1.20	0.44			

8	Au/2	5.532	1.67	1.18	0.48

The trace of the transition density matrix is the measure of the number of electrons excited in forming a given excited state. The shapes of the orbitals corresponding the 1-TRDM largest singular values are shown in figures listed below. The semi-transparent pink/pumpkin surface corresponds to the "leaving" orbital of the 1Ag ground state. The solid blue/turquose orbital shows the "accepting" orbital of the excited state. The number of electrons transferred for each orbital pair is the singular value.

Note that none of the seven low-lying excited states in this system are of a simple one-electron character. The two lowest excited states are of a significant triple-excited character [as noted previously by Rubio et al]. The five lowest excited states are of a pi->pi* character. Excitation to the S1 (1Bu) involves transfer of 1.2 electrons from the ring pi systems to the central C=C pi bond, which is expected to cause a significant shortening and stiffening of this bond. In contract, formation of the S_2 (2Ag) excited state involves primarily rearrangement of the electron density within the ring pi system. As a result, it is expected to undergo a slight ring expansion. This state has a pronounced bi-radical character, with two excitations being equally important. The S_3 (3Ag) state is of a similar nature, but involves weakening of a C4-C5 double bond, instead of the S1-C5 bond for the S_2. The second dipole allowed excitations (S_4, 2Bu) and the nearby S_5 (4Ag) are dominated by transfer of an electron from the sulfur P_z orbital to the central C=C bond. Finally, the quasi-degenerate S_6 (1Bg) and S_7 (1Au) states correspond to a transfer of an electron from the pi orbitals to the vacant d orbitals of the sulfur atom, stabilized by a partial sigma bond to the carbon atoms.

2. Electronic structure of 2TSO

The final active space of 2TSO molecule consisted of a 7-orbital occupied block (3*Au + 1*Ag + 3*Bg irreducible representations) and a 12-orbital virtual block (3*Au + 3*Ag + 3*Bg + 3*Bu). The active space was optimized for the 20 equally-weighted singlet states. For a comparison, we also show the results from a calculation using a smaller 9-orbital virtual block (3*Au + 1*Ag + 3*Bg + 2*Bu) and averaging over 15 lowest singlet states.

Unfortunately, it has proven impossible to repeat the calculation using the cc-pVTZ basis set. Judging by the 2T results, the basis set corrections to the cc-pVDZ results should not exceed 0.5 eV.

The lowest singlet excited states of 2TSO are (in eV).

16-orbital active space

		MCQDPT2	MCSCF	##	Osc.Str.
1	Ag/1	0.000	0.000	1	
2	Bu/8	3.892	7.989	10	0.3049
3	Ag/12	3.910	7.980	9	
4	Bu/3	4.047	5.232	3	1.1908
5	Ag/3	4.326	4.362	2	
6	Au/2	4.766	7.035	7	0.0033
7	Ag/5	5.182	6.270	5	
8	Bu/5	6.046	6.053	4	0.0061
9	Bg/2	6.118	8.662	13	
10	Ag/13	6.148	8.747	15	
11	Bu/12	6.712	8.665	14	0.0757
12	Ag/10	7.454	7.477	8	

13	Au/4	7.464	8.123	11	0.0004
14	Ag/7	7.813	6.762	6	
15	Bu/10	8.356	8.340	12	0.0178

19-orbital active space

		MCQDPT2	MCSCF	##	Osc.Str.
1	Ag/1	0.000	0.000	1	
2	Ag/12	3.662	7.808	9	
3	Bu/8	3.915	7.808	10	0.6388
4	Bu/3	4.035	5.133	3	0.8287
5	Ag/3	4.358	4.384	2	
6	Au/2	4.937	7.186	7	0.0004
7	Ag/5	5.318	6.187	5	
8	Bu/17	5.448	9.554	18	0.0758
9	Ag/17	5.750	9.540	17	
10	Bg/3	6.166	8.752	15	
11	Bu/5	6.242	6.082	4	0.0064
12	Ag/13	6.482	8.627	14	
13	Bu/12	6.764	8.617	13	0.0219
14	Au/4	7.676	7.837	11	0.0004
15	Bu/18	7.680	9.742	20	0.0330
16	Ag/8	7.961	6.793	6	
17	Bg/4	8.339	8.827	16	
18	Ag/10	8.512	7.486	8	
19	Bg/6	9.390	9.576	19	
20	Bu/10	9.893	8.354	12	0.0212

The ordering of the low-lying states is in a good agreement for the two active spaces, with only two interchanges occuring among the lowest ten states (S_1/S_2 and S_8/S_9).
The MCQDPT2 excitation energies for the lowest ten states also agree closely, with the largest change (0.6 eV) found for S_7 (3Bu) state. As a result, the 19-orbital active space calculation may be expected to be converged with respect to the treatment of electron correlation.

Unlike in the 2S molecule, where the S_1 was an isolated pi->pi* 1Bu state, 2TSO has a nearly degenerate S_1 and S_2 states. At the highest correlation treatment level used here, the 2Ag state appears to be the S_1. However, since it is separated from the dipole-allowed 1Bu in S_2 by only 0.25 eV, the ordering of the two states could change with further improvements in the basis set and correlation treatment.

The transition density matrices for the MCSCF wavefunctions corresponding to the ten lowest states of 2TSO are summarized below:

	State	MCQDPT2	1-TRDM trace	1-TRDM singular values > 0.1				
				1	2	3		
1	Ag/1	0.000						
2	Ag/12	3.662	1.97	1.01	0.43	0.18	0.10	
3	Bu/8	3.915	1.94	1.15	0.53			
4	Bu/3	4.035	2.10	1.27	0.33	0.19		
5	Ag/3	4.358	1.53	0.70	0.54			
6	Au/2	4.937	1.55	1.30	0.11			
7	Ag/5	5.318	2.41	0.93	0.91	0.14	0.12	0.12
8	Bu/17	5.448	2.26	0.93	0.55	0.34	0.15	
9	Ag/17	5.750	1.94	1.07	0.43	0.15		
10	Bg/3	6.166	1.94	1.18	0.45	0.22		
11	Bu/5	6.242	1.57	0.67	0.49	0.16		

The two lowest states of 2TSO (2Ag and 1Bu) involve transfer of an electron from the sulfoxide oxygen atom to the pi system. The transferred electron populates C3=C4, C5=C5' and C3'=C4' double bonds. For both S_1 and S_2, the pattern of the electron transfer is nearly identical, with the only significant difference being the relative phases of the donor p orbitals on the sulfoxide fragments. As a result, these two states should remain near-degenerate upon improvements in the basis sets and correlation treatment. The similar observation applies to the S_7 (3Bu) and S_8 (5Ag) pair. These two states again arise from sulfoxide-O to a higher-lying pi* orbital, and should remain as a quasi-degenerate state pair.

The next two excited states - 2Bu (S_3) and 3Ag (Ag) are pi->pi* transitions, dominated by a "flip" in the double bond character along the linear C2-C3-C4-C5-C5'-C4'-C3'-C2' conjugated chain. The acceptor orbitals of the two states are closely related to the S_4 and S_5 in the 2T molecule. However, since the p orbital of the sulfur is no longer available for conjugation, the electron is supplied by the carbon-based pi orbitals in 2TSO, instead of the sulfur p_z orbitals in 2T. In a way, S_3 and S_4 states of 2TSO illustrate the polyacetylene-like nature of the 2TSO aromatic system, with electron delocalization proceeding along the one-dimensional carbon chain.

The next excited state in 2TSO - the 1Au S_5 - and its 1Bg counterpart (S_9) has no direct counterpart in 2T again. The presence of the strongly electron-withdrawing sulfoxide groups causes destabilization of the sulfur-carbon bonds, reducing the energy needed for these sigma->pi* excitations.

Finally, the 4Ag S_6 in 2TSO is the direct analog of S_3 in 2T, while the S_6 (1Bg) and S_7 (1Au) of the 2T molecule have no analog in 2TSO due to the lack of non-bonding sulfur lone pairs in this molecule.

One might expect similar observations to apply to longer oligomers of S,S-dioxide thiophenes. The lowest excited state manifold in these systems may be expected to come from the O(n) to pi* excitations. Due to the lack of direct interaction between the =SO2 fragments, dipole-allowed states in this manyfold could be expected to be accompanied by optically dark gerade counterparts. Thus, the =SO2 fragment serves as a more effective functional analog of the sulfur p_z orbitals in the thiophene ologimers (cf. S_1/S_2 in 2TSO and S_4/S_5 in 2T).

The ability of the thiophene p_z orbitals into act as a pure electron dopant in oligo-T is impaired by the residuals conjugation to the carbon-centered pi system. Due to the mismatch in the size of the orbitals, the oligo-TSO =SO2 fragment is essentially unable to participate in the pi-system conjugation. As a result, the second excited-state manifold in oligo-TSO acquired a nearly pure oligoene character, with a set of one-dimensional pi->pi* states appearing in this molecule. The pi->pi* states in oligo-T are of a more complex nature due to multi-path interference causes by participation of sulfur p_z orbitals (cf. S_3/S_4 in 2TSO and S_1/S_2 in 2T).

References:

[GAMESS] a) M.W.Schmidt, K.K.Baldridge, J.A.Boatz, S.T.Elbert, M.S.Gordon, J.J.Jensen, S.Koseki, N.Matsunaga, K.A.Nguyen, S.Su, T.L.Windus, M.Dupuis, J.A.Montgomery J.Comput.Chem. 14, 1347-1363 (1993); b) M.S.Gordon, M.W.Schmidt pp 1167-1189 in "Theory and Applications of Computational Chemistry, the first forty years" C.E.Dykstra, G.Frenking, K.S.Kim, G.E.Scuseria (editors), Elsevier, Amsterdam, 2005.

[ORMAS] J.Ivanic J.Chem.Phys. 119, 9364-9376, 9377-9385(2003).

[MCSCF] (FULLNR converger) G.D.Fletcher, Mol.Phys. 105, 2971-2976(2007).

[MCQDPT2] a) H.Nakano, R.Uchiyama, K.Hirao, J.Comput.Chem. 23, 1166-1175(2002); b) M.Miyajima, Y.Watanabe, H.Nakano J.Chem.Phys. 124, 044101/1-9(2006); c) R.Ebisuzaki, Y.Watanabe, H.Nakano Chem.Phys.Lett. 442, 164-169(2007).

[Rubio] M. Rubio, M. Merchan, E. Orti, J.Chem.Phys. 102, 3580 (1995)